Journal of Magnetism and Magnetic Materials 321 (2009) 2601–2606

Contents lists available at ScienceDirect

Journal of Magnetism and Magnetic Materials

journal homepage: www.elsevier.com/locate/jmmm

Electron-doped $Sm_{1-x}Sr_xMnO_3$ perovskite manganites: Crystal and magnetic structures and physical properties

A.I. Kurbakov [a,*], C. Martin [b], A. Maignan [b]

[a] Petersburg Nuclear Physics Institute of the Russian Academy of Sciences, 188300 Gatchina, Leningrad Region, Russia
[b] Laboratoire CRISMAT, UMR 6508 ENSICAEN et Université de Caen, Bd. du Maréchal Juin, 14050 Caen, France

ARTICLE INFO

Article history:
Received 26 May 2008
Received in revised form
24 February 2009
Available online 25 March 2009

PACS:
75.47.Lx
75.25.+z
61.12.Ld

Keywords:
Magnetism
Manganite
Crystal and magnetic structure
Neutron diffraction

ABSTRACT

We present the results of a study of electron-doped $Sm_{1-x}Sr_xMnO_3$ ($x>0.5$) perovskite manganites by combining high-resolution neutron powder diffraction with measurements of resistivity, magnetization and magnetic susceptibility. Although investigated $Sm_{0.45}Sr_{0.55}MnO_3$ and $Sm_{0.37}Sr_{0.63}MnO_3$ compounds belonging to the same phase diagram area differ significantly in the strontium content, they are homogeneous antiferromagnetic (AF) insulators and do not exhibit CMR. They have different crystallographic symmetries (orthorhombic *Pbnm* and tetragonal *I4/mcm*, respectively) in the entire temperature range under study (1.5–288 K), differ in the type of spin ordering at low temperatures (AF-*A* and AF-*C*), are characterized by different orbital polarizations ($d_{x^2-y^2}$ and $d_{3z^2-r^2}$), and possess two- and one-dimensional magnetic properties, respectively. The lack of magnetoresistance for these compositions is explained by the lack of coexisting magnetic phases involving double exchange ferromagnetism, in contrast to what is observed for the magnetoresistive $Sm_{1-x}Sr_xMnO_3$ compounds, that is with $x\leqslant 0.52$.

1. Introduction

Studies of manganites of the general formula $R_{1-x}A_xMnO_3$ (where R is a lanthanide and A is an alkaline-earth or any other divalent metal) are motivated by their rich phase diagrams exhibiting a variety of phases with unusual types of magnetic, structural, or electronic ordering. The asymmetry of the magnetic and transport properties between hole- and electron-doped perovskite manganites partly results from their different concentrations of Jahn–Teller Mn^{3+} cations. Depending on the actual concentration x of the element A, the physical properties of manganites can vary noticeably with a change in the temperature and external magnetic field, which, in turn, can induce sequences of phase transitions [1–3]. The present report is a continuation of our systematic physical investigation of the $Sm_{1-x}Sr_xMnO_3$ manganites [4–9], which are of considerable research interest [3,10–12]. Owing to the large difference between the ionic radii of samarium and strontium the $Sm_{1-x}Sr_xMnO_3$ manganites exhibit, with a rather typical behavior for manganites, unique physical properties with a vivid manifestation of interactions between the electron, phonon, and magnetic subsystems. The previous systematic investigations of $Sm_{1-x}Sr_xMnO_3$ ceramic samples by measuring the temperature and field dependences of the resistivity and magnetization [3] demonstrated that colossal magnetoresistance (CMR) effect manifests itself mainly in the range of hole doping, for $0.3\leqslant x\leqslant 0.52$, with a maximum at $x=0.44$. These data were confirmed later by similar investigations on single crystals [10]. In this paper, two different ranges were found in the diagram for compositions with $x\geqslant 0.5$. In the concentration region $0.5\leqslant x\leqslant 0.575$, a pure antiferromagnetic (AF) state without a spontaneous magnetization is observed below the Néel temperature T_N, whereas an additional low-temperature magnetic transition to a new phase exhibiting a weak non-zero ferromagnetic moment was revealed in the second range ($0.60\leqslant x\leqslant 0.67$). In view of the above considerations, we found important to supplement the previously obtained neutron diffraction data on hole-doped $Sm_{1-x}Sr_xMnO_3$ ($x<0.5$) with data on electron-doped manganites having values of x, beyond the threshold corresponding to the change in the sign of carriers near the region where the CMR effect exists. On the basis of previous discussion, the two compounds $Sm_{0.45}Sr_{0.55}MnO_3$ and $Sm_{0.37}Sr_{0.63}MnO_3$ were selected ($x=0.55$ and $x=0.63$) for investigations.

2. Experimental

2.1. Preparation and certification of the sample

To suppress the very strong neutron absorption by the ^{149}Sm isotope presents in natural samarium, the samples for neutron

* Corresponding author. Tel.: +7 8137146954; fax: +7 8137130173.
E-mail address: kurbakov@pnpi.spb.ru (A.I. Kurbakov).

0304-8853/$ - see front matter © 2009 Elsevier B.V. All rights reserved.
doi:10.1016/j.jmmm.2009.03.040

diffraction analysis were synthesized using the ^{152}Sm isotope. The $^{152}Sm_{0.45}Sr_{0.55}MnO_3$ and $^{152}Sm_{0.37}Sr_{0.63}MnO_3$ samples have been prepared by using a conventional synthesis process in air [13]. Stoichiometric ratios of $^{152}Sm_2O_3$, $SrCO_3$, and MnO_2 were weighted, mixed, and heated in air 12 h at 1000 °C. These powders were then crushed and pressed in the form of bars and synthesized in two steps at 1200 and 1500 °C during 12 h with a slow cooling down to 800 °C. The purity of the samples was checked by X-ray powder diffraction at room temperature. A lot of crystallites of the prepared samples were tested by electron diffraction. The cationic composition was determined by energy dispersive spectroscopy analysis, showing that the cationic distribution is homogeneous and that the real composition is identical to the nominal one.

2.2. Macroscopic measurements

Electrical resistances were measured, decreasing the temperature, with the four-probe technique in a PPMS, Quantum Design, that also allows magnetic field scans. The magnetic susceptibility values were calculated using the magnetization data collected in a MPMS, Quantum Design, SQUID magnetometer. The measurements were taken in an external magnetic field of 100 Oe in the temperature range $T = 5$–400 K after cooling of the sample in the field (FC) and without a field (ZFC). Isothermal measurements were also made at 5 K by varying the magnetic field between 0 and 5 T.

2.3. Neutron powder diffraction

The neutron diffraction measurements were performed on the Russian–French 7-section high-resolution neutron powder diffractometer G4.2 equipped with 70 counters that was installed on a cold neutron guide of the Orphée reactor (Léon Brillouin Laboratory, Saclay, France) [14]. Neutron diffraction patterns were measured in the superposition mode using monochromatic neutrons with a wavelength $\lambda = 2.3428$ Å in the angular range $3° \leqslant 2\theta \leqslant 140°$ upon heating at several temperatures from 1.5 to 288 K in a cryofurnace. The particular temperatures were chosen to provide measurements in different regions of the phase diagram in accordance with the results obtained in [3,10] and the goals pursued in our macroscopic measurements with the samples under study. The Rietveld analysis of the neutron diffraction data was performed by using the Fullprof suite [15].

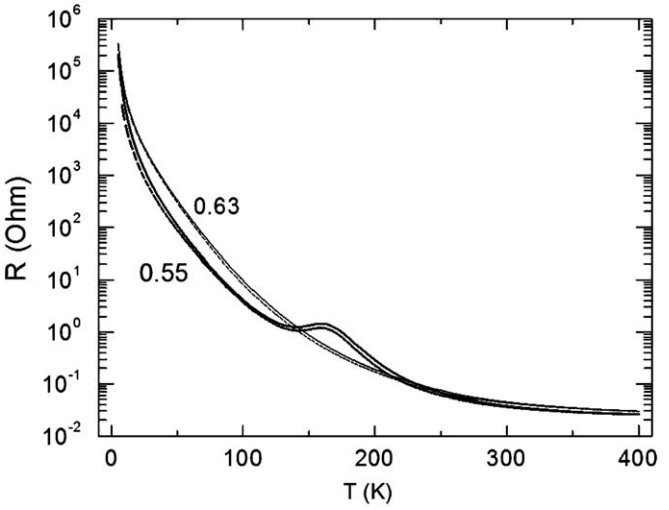

Fig. 1. Temperature dependences of the electrical resistivity of the $Sm_{0.45}Sr_{0.55}MnO_3$ and $Sm_{0.37}Sr_{0.63}MnO_3$ compounds in 0 (continuous lines) or 7 T (dashed lines).

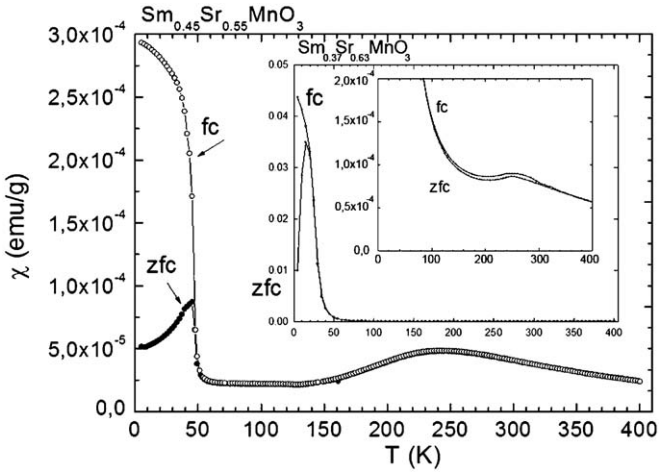

Fig. 2. Temperature dependences of the *ac* magnetic susceptibility of the $Sm_{0.45}Sr_{0.55}MnO_3$ and $Sm_{0.37}Sr_{0.63}MnO_3$ (inset) compounds in an external magnetic field of 100 Oe upon cooling without a field (ZFC) and in the field (FC). The fragment of the dependences of $Sm_{0.37}Sr_{0.63}MnO_3$ is submitted also on an enlarged scale.

3. Experimental results

3.1. Macroscopic measurements

The temperature dependences of the resistivity of both samples (Fig. 1) demonstrate the absence of clear metal–insulator (MI) transition, which is characteristic of $Sm_{1-x}Sr_xMnO_3$ manganites exhibiting CMR. The samples remain insulators throughout the temperature range covered, without dependence from the applied magnetic field (up to 7 T). However, $\rho(T)$ curves of $Sm_{0.45}Sr_{0.55}MnO_3$ exhibit a maximum for $T \approx 160$ K indicating a more conducting regime below this temperature. This local resistivity maximum is attributed to the metallic character of the ferromagnetic (*F*) planes of the *A*-type antiferromagnetic (AF-*A*) structure that takes place around this temperature.

The absence of ferromagnetic ordering is confirmed by the isothermal magnetic field-dependent magnetization curve for $Sm_{0.45}Sr_{0.55}MnO_3$ (not shown). These $M(H)$ curves collected at 2.5 and 5 K reveal maximal magnetization values reaching only $\cong 0.16\,\mu_B$/Mn in 7 T, i.e. much lower than expected for a fully saturated ferromagnetic order ($\cong 3.45\,\mu_B$/Mn). Furthermore, instead of a tendency towards saturation, these curves exhibit a faster increase of magnetization for $H > 4$ T characteristic of the beginning of a smooth metamagnetic transition.

The temperature dependences of the magnetic susceptibility for both compounds displayed in Fig. 2 also support the absence of important ferromagnetic component at low temperatures. Nevertheless, one observes an abrupt transition at 50 and 20 K, for $Sm_{0.45}Sr_{0.55}MnO_3$ and $Sm_{0.37}Sr_{0.63}MnO_3$, respectively, with a difference in the FC and ZFC magnetic susceptibility curves. Another characteristic feature in the susceptibility measurements is a kink in FC and ZFC curves in the range of 250 K. But it is important to note that the character of these kinks differs for both samples.

As shown in the Fig. 3 for inverse susceptibility against *T*, no linear regime is reached up to 400 K (or in a too small temperature range) to extract reliable effective magnetic moments.